Synthetic Metals 228 (2017) 41–44

Contents lists available at ScienceDirect

Synthetic Metals

journal homepage: www.elsevier.com/locate/synmet

Interfacial and space charge dielectric effects in Polypyrrole/Zinc Oxide composites

A.N. Papathanassiou[a,*], I. Sakellis[a], E. Vitoratos[b], S. Sakkopoulos[b]

[a] National and Kapodistrian University of Athens, Physics Department, Panepistimiopolis, 15784 Zografos, Athens, Greece
[b] University of Patras, Physics Department, 28500 Patras, Greece

ARTICLE INFO

Keywords:
Zinc oxide
Polypyrrole
Composites
Permittivity

ABSTRACT

Polypyrrole/zinc oxide composites were studied by broadband dielectric spectroscopy in the frequency range 10 mHz to 1 MHz for temperature ranging from 15 K to room temperature. Lowering temperature, the dc conductivity was suppressed, revealing underlying dielectric relaxation mechanisms. For pristine polypyrrole and 10 wt% ZnO composites, no dielectric relaxation is detectable. For 20, 30 and 40 wt% ZnO composites, a relaxation was detected in the vicinity of range 10^4–10^5 Hz. Its typical mean relaxation time and its concentration dependence are compatible with Sillar's model for interfacial polarization in heterogeneous matter consisting of inclusions dispersed within a dielectric matrix. At high ZnO concentration, a low-frequency relaxation also appeared around 0.01–10 Hz, stemming from space charge polarization. The shift of the relaxation upon temperature provides an insight to the dynamics of relaxing charge entities.

1. Introduction

Electron conducting polymers have been studied extensively for the past years [1–3] and as well as novel well-characterized metallic or semi-conducting polymers, blends and composites [4–10]. Broadband dielectric spectroscopy is a powerful tool for studying electric charge flow of different scale and capacitance effects over a broad frequency range [11–15]. Carriers created in polypyrrole (PPy) by photo-excitation recombine much faster than those produced in inorganic semiconductors. Polymer/inorganic semiconductor composites can achieve tunable electro-optical properties upon composition: photo-generated excitons are dissociated at the polymer/inorganic semiconductor interface with electrons and holes being transferring to the inorganic and to the polymer phases, respectively. ZnO is a transparent metal oxide, with a direct energy gap of about 3.4 eV (which is comparable to a 2.4 eV energy gap for PPy). In the UV range because of electron excitations from the top of the valence band to the bottom of the conduction band and exhibits a high exciton coherence (60 eV), is bio-compatible and requires low-cost easy manufacturing. Metal oxides do not merely blend with a conducting polymer, but they are encapsulated in it improving its physical properties and making it suitable for diverse applications [16], e.g. solar cells [17], fuel cells [18], chromatic sensors [19], microwave absorption layers [4], etc. In conducting polymers and composites, the dc-conductivity is intense to mask capacitance and dielectric loss effects. Hopping conductivity depends upon temperature more strongly than dielectric relaxation mechanisms do. Hence, a simple method to achieve detection of relaxation related to capacitance effects is by cooling the specimen.

2. Experimental

The procedure for sample preparation, which was reported earlier [20], is the following, in brief: PPy/ZnO x% (w/w) composites, with x = 10, 20, 30 and 40, were prepared by freshly distilled pyrrole (Merc) under a vacuum, mixed with the proper amount of ZnO powder and polymerized in the presence of $FeCl_3$ as an oxidant (monomer/oxidant = 1:1 mol/mol) in HCl acid–water solutions at pH 2.00 in an ice bath under a nitrogen atmosphere. The ZnO powder had particles in the range 50–300 nm. The composites in the form of black powders were dried for 24 h and then compressed in an IR press under a 10 t/cm^2 pressure for about 15 min. By this way disk-shaped specimens of about 13 mm in diameter and 1.5 mm thick were obtained. XRD spectra and SEM images indicated that ZnO particles are completely embedded into PPy [20,21].

The diameter of the disk-shaped specimens was 13 mm and the thickness was about 1.5 mm. The parallel surfaces of the samples were silver pasted to ensure good electrical contact with electric probes. The specimen was placed in a capacitor type sample holder of a high-vacuum liquid helium cryostat (ROK, Leybold-Hereaeus) operating from 15 K to room temperature. Temperature was stabilized with an

* Corresponding author.
E-mail address: antpapa@phys.uoa.gr (A.N. Papathanassiou).

http://dx.doi.org/10.1016/j.synthmet.2017.03.019
Received 20 December 2016; Received in revised form 29 March 2017; Accepted 29 March 2017

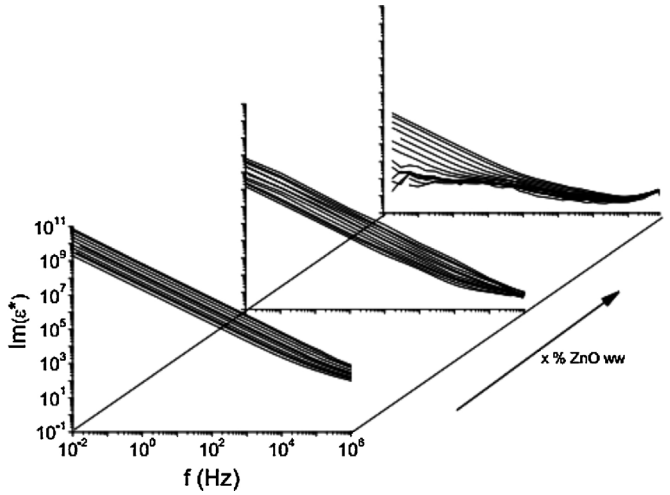

Fig. 1. Typical isotherms of the imaginary part of the complex permittivity against frequency for 20, 30 and 40 wt% ZnO composites (top to bottom diagrams, respectively). In each diagram, isotherms range from room temperature to 15 K (from upper to lower curves, respectively).

accuracy of 0.01 K by a LTC-60 temperature controller. Complex permittivity measurements were performed in the frequency range between 1 mHz and 1 MHz with a Solartron SI 1260 Gain-Phase Frequency Response Analyzer, and a Broadband Dielectric Converter (BDC, Novocontrol). Data were collected by employing the WinDeta (Novocontrol) software [22,23].

3. Results and discussion

The complex permittivity ε^* was studied in the frequency domain (from 1 mHz to 1 MHz) at various temperatures ranging from the 15 K to room temperature. Isotherms of the measured imaginary part of the dielectric constant vs frequency at room temperature for PPy and PPy/ZnO are depicted in Fig. 1. The spectra of PPy and PPy/10 wt% ZnO, are described by $\mathrm{Im}(\varepsilon^*) = \sigma_0/\varepsilon_0 2\pi f^n$, where σ_0 denotes the dc conductivity, ε_0 is the permittivity of free space and n is a fractional exponent. Fitting the last equation to the isothermal data points, σ_0 and n are obtained (n was found to be equal to 1). On increasing the ZnO loading, a broad dielectric loss mechanism appears in the high-frequency. Above 10 wt% ZnO, dielectric relaxation mechanism close to 10^5 Hz (HF relaxation) appears. In the upper frequency limit, a tail of another relaxation peak was positioned beyond the frequency range of our instrumentation and cannot be explored in the present study. For 30 and 40 wt% ZnO composites an additional strong relaxation has its maximum around 0.1–10 Hz (LF relaxation); its time scale (roughly reciprocal to the maximum frequency f_{max}) is quite large (roughly 0.1–10 s) and typical for space charge relaxation in poor semi-conductors and insulators. Isotherms were fitted by:

$$\mathrm{Im}(\varepsilon^*) = \frac{\sigma_0}{\varepsilon_0 2\pi f^n} + \frac{\Delta\varepsilon_{LF}}{(1 + (f/f_{0,LF})^{a_{LF}})^{b_{LF}}} + \frac{\Delta\varepsilon_{HF}}{(1 + (f/f_{0,HF})^{a_{HF}})^{b_{HF}}} \quad (1)$$

where the subscripts LF and HF refer to the above mentioned relaxation mechanisms, respectively, $\Delta\varepsilon$ is the intensity of the relaxation mechanism, a and b are fractional exponents related to the width and the asymmetry of a relaxation peak and f_0 is a parameter that coincides with the peak maximum frequency f_{max}, provided that $b = 1$. Each relaxation peak is assumed to obey the Harviliak–Negami (H–N) model [24], where a ($0 < a \leq 1$) and b ($0 < b \leq 1$) [25,26].

The contribution of the first term of the sum appearing in Eq. (1) becomes weaker on cooling and, subsequently, dielectric relaxation mechanisms, appearing as 'knees' in log–log plots of $\mathrm{Im}(\varepsilon^*)$ vs frequency (Fig. 1) are revealed. At least one dielectric loss peak is detected (one is beyond the available upper frequency limit). In the present work, we shall only refer to relaxations within the working frequency range of the available instrumentation. In Fig. 2, typical fits of Eq. (3) to the data points collected at a given temperature for 20, 30 and 40 wt% ZnO composites are presented. The frequency f_{max}, where a relaxation peak has its maximum, is plotted as a function of reciprocal temperature and is presented in Fig. 3. Relaxation HF is activated around 105 Hz and appears in 20, 30, 40 wt% ZnO composites, while relaxation LF is detected in 30 and 40 wt% ZnO composites appears around 10 Hz. $\log f_{max}$ vs reciprocal temperature of relaxations HF and LF, respectively, are depicted in Fig. 3.

The variation of composition has little effect on the position of relaxation HF. PPy/ZnO composite can be described approximately as an heterogeneous system consisting of the matrix (phase D) and randomly dispersed spheres (phase S). The inter-sphere spacing is assumed to be larger than the sphere's radius. Labeling σ_j and ε_j, the dc conductivity and the relative dielectric constant, respectively, of

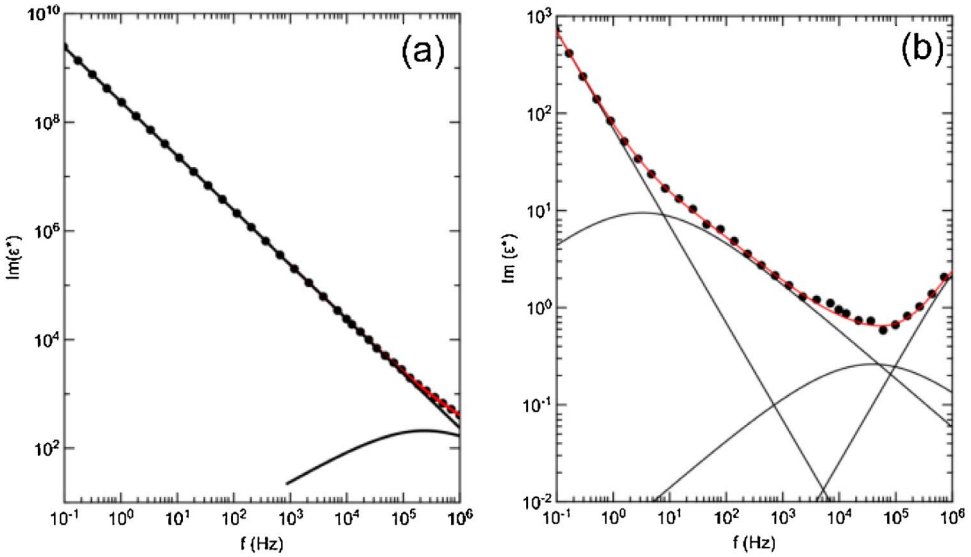

Fig. 2. Best fit of Eq. (1) to the data points collected at: (a): 205 K for 20 and (b): 40 wt% ZnO composite, respectively. Straight line is the dc conductivity contribution. The components of the fitting curves, straight lines and H–N relaxation peaks are also shown. Both spectra indicate the HF relaxation. The fitting parameters are: (a): $\log \sigma_0 = -3.874$ (σ_0 in S/cm), $n = 1.000$, $\log f_0 = 5.63$ (f_0 in Hz), $\Delta\varepsilon = 422$, $a = 1$, $b = 1$; (b): $\log \sigma_0 = -9.696$ (σ_0 in S/cm), $n = 0.998$, $\log f_0 = 1.34$ (f_0 in Hz), $\Delta\varepsilon = 422$, $a = 0.5$, $b = 1$ (left peak), $\log f_0 = 4.76$ (f_0 in Hz), $\Delta\varepsilon = 1.3$, $a = 0.5$, $b = 1$ (middle peak); the left peak positioned beyond the upper measuring frequency limit has been added to match the high frequency tail.

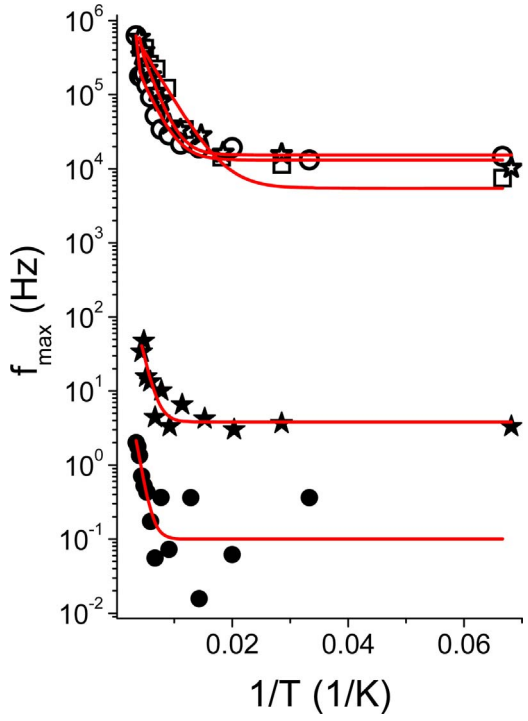

Fig. 3. Log f_{max} against reciprocal temperature for LF (solid symbols) and HF relaxation, respectively. Circles, squares and stars correspond to 20, 30 and 40 wt% ZnO composites, respectively.

Table 1
Fit parameters of Eq. (3) for relaxations LF and HF, respectively.

ZnO (wt%)	Relaxation	Parameters of Eq. (3)		
		A (s^{-1} K^{-1})	C (s^{-1})	E (eV)
20	HF	53	1.5×10^6	0.03
30	LF	0.04	2.1×10^3	0.09
	HF	406	1.0×10^7	0.07
40	LF	92	0.9×10^2	0.105
	HF	557	4.7×10^{10}	0.29

phase j (j = M, S), the relaxation time τ for interfacial polarization due to electric heterogeneity of the composite, has been estimated by Sillars [27]:

$$\tau = \frac{\varepsilon_0[2\varepsilon_M+\varepsilon_S - \upsilon_S(\varepsilon_S - \varepsilon_M)]}{[2\sigma_M+\sigma_S - \upsilon_S(\sigma_S - \sigma_M)]} \quad (2)$$

where υ_S denotes the volume fraction of the dispersed phase. Conducting PPy is the matrix (phase M) and ZnO is the dispersed phase (phase S). Dc conductivity values of un-doped ZnO distribute around a mean value $\sigma_S \approx 0.4$–6×10^{-3} S/m and a typical dielectric constant value is $\varepsilon_M \approx 10^4$ [28]. For conducting PPy, $\sigma_M \approx 10^{-1}$ S/m and $\varepsilon_M \approx 10^4$. Using these values, which imply that $\sigma_M \gg \sigma_S$ and $\varepsilon_M \gg \varepsilon_S$, Eq. (2) predicts the corresponding relaxation has its maximum approximately around $f_{max} \equiv \tau^{-1}$ and is practically independent on ZnO loading. Both predictions about the location of the relaxation and its weak sensitivity on composition are consistent with the experimental results. Furthermore, by replacing the above mentioned typical values into Eq. (2), we get $f_{max} \approx 7 \times 10^5$ Hz, which practically coincides with the maximum frequency of relaxation HF.

The temperature dependence of f_{max} is depicted in Fig. 3. Consider the model of an electron of mass m relaxing between two neighboring potential wells by phonon assisted tunneling through a potential barrier of height u and width δ. The corresponding maximum frequency f_{max} consists of a linear low-temperature single phonon term and, at higher temperature, an exponential multi-phonon hopping term:

$$f_{max}(T) = AT + C\exp\left(-\frac{E}{kT}\right) \quad (3)$$

where the parameters $A = 2\nu\exp\left\{\left(\frac{\hbar^2}{8\delta^2 mu}\right)^{1/2}\right\}\left(\frac{2\delta^2 m}{\hbar^2 u}\right)^{1/2} k$, $\hbar$ is the Planck's constant and ν denotes the vibrational frequency and C are practically temperature independent [29–31]. Best fits of Eq. (3) to the data points depicted in Fig. 3 are shown as solid lines. The fitting parameters are enlisted in Table 1.

The values of all fitting parameters for relaxation HF increase systematically on ZnO content. More specifically, the increase of the activation energy indicates that locally relaxing charges sense a less conducting environment as the composite becomes richer in ZnO. This visualization is in agreement with the decrease of the dc conductivity on ZnO and the gradual transition from a semi-conducting state to an insulating one, respectively. Relaxation LF is sensitive to the electrode material, which typically characterizes space charge phenomena, resulting from the non-ohmic sample-electrode contact.

4. Conclusions

Below 20 wt% ZnO, PPy/ZnO composites behave as loss free semiconductors in the frequency range 10 mHz to 1 MHz and temperatures ranging from 15 K to room temperature. For 20, 30 and 40 wt% ZnO composites, a high frequency relaxation has its maximum frequency within 10^4–10^5 Hz. Its characteristic mean relaxation time and its concentration dependence are compatible with the theory for interfacial polarization in dispersions. For 30 and 40 wt% ZnO composites, an additional space charge relaxation appears around 10^{-2} to 10 Hz. The dependence of the relaxation mechanisms upon temperature indicates a low temperature single phonon assisted hopping and, at higher temperature, multi-phonon hopping, respectively. Composites loaded equal or less than 10 wt% ZnO combine good electrical conduction, poor capacitance effects and sufficient ohmic sample-electrode contacts.

References

[1] K. Lee, A.J. Heeger, Phys. Rev. B 68 (2003) 035201.
[2] V.N. Prigodin, A.J. Epstein, Synth. Met. 125 (2002) 43.
[3] A.N. Papathanassiou, I. Sakellis, J. Grammatikakis, Appl. Phys. Lett. 91 (2007) 202103.
[4] A.B. Kaiser, V. Skákalová, Chem. Soc. Rev. 40 (2011) 3786.
[5] A.B. Kaiser, Adv. Mater. 13 (2001) 927.
[6] P. Jayakrishnan, M.T. Ramesan, Mater. Chem. Phys. 186 (2017) 513.
[7] P. Jayakrishnan1, M.T. Ramesan, J. Inorg. Organomet. Polym. 27 (2017) 323.
[8] K. Jayakrishnan, A. Joseph, J. Bhattathiripad, M.T. Ramesan, K. Chandrasekharan, N.K. Siji Narendran, Opt. Mater. 54 (2016) 252.
[9] M.T. Ramesan, K. Surya, J. Appl. Polym. Sci. 133 (2016) 5431.
[10] M. Dinari, P. Asadi, RSC Adv. 5 (2015) 60745.
[11] A.N. Papathanassiou, I. Sakellis, J. Grammatikakis, S. Sakkopoulos, E. Vitoratos, E. Dalas, Synth. Met. 42 (2004) 81.
[12] A.N. Papathanassiou, J. Grammatikakis, I. Sakellis, S. Sakkopoulos, E. Vitoratos, E. Dalas, J. Appl. Phys. 96 (2004) 3883.
[13] E. Singh, A.K. Narula, R.P. Tandon, A. Mansingh, S. Chandra, J. Appl. Phys. 80 (1996) 985.
[14] S. Capaccioli, M. Lucchesi, P.A. Rolla, G. Ruggeri, J. Phys. Condens. Matter 10 (1998) 5595.
[15] P. Dutta, S. Biswas, K.D. De, J. Phys. Condens. Matter 13 (2001) 9187.
[16] A.N. Papathanassiou, J. Grammatikakis, I. Sakellis, S. Sakkopoulos, E. Vitoratos, E. Dalas, Appl. Phys. Lett. 87 (2005) 154107.
[17] K.S. Narayan, Handbook of polymers, in: D. Bansi, Malhota (Eds.), Electronics, Rapra Technology Ltd, Shawbury, UK, 2002, pp. 341–365.
[18] H.Y. Chang, C.W. Lin, J. Membr. Sci. 218 (2003) 295.
[19] Shimada, K. Ookubo, N. Komuro, Y. Shimizu, N. Uehara, Langmuir 23 (2007) 11225.
[20] E. Dalas, P. Mougoyannis, S. Sakkopoulos, Rom. J. Physiol. 58 (2013) 354.
[21] S. Sakkopoulos, E. Vitoratos, E. Dalas, Ch. Anestis, P. Mougoyannis, J. Surf. Interfaces Mater. 2 (2014) 328.
[22] A.N. Papathanassiou, M. Plonska-Brzezinska, O. Mykhailiv, L. Echegoyen, I. Sakellis, Synth. Met. 209 (2015) 583.
[23] A.N. Papathanassiou, O. Mykhailiv, I. Sakellis, L. Echegoyen, M. Plonska-Brzezinska, J. Phys. D Appl. Phys. 49 (2016) 285305.

[24] E. Kremer, A. Schonhals, Broadband Dielectric Spectroscopy, Springer-Verlag, Berlin-Heidelberg/New York, 2003 (Chapter 1).
[25] S. Havriliak, S. Negami, J. Polym. Sci. C 14 (1966) 89.
[26] R.H. Cole, K.S. Cole, J. Chem. Phys. 9 (1941) 341.
[27] L.K.H. van Beek, J.B. Birks (Ed.), Dielectric Behavior of Heterogeneous Systems in Progress in Dielectrics, vol. 7, Heywood, London, 1967, pp. 71–114.
[28] A.Y. Polyakov, N.B. Smirnov, A.V. Govorkov, E.A. Kozhukhova, S.J. Pearton, D.P. Norton, A. Osinsky, A. Dabiran, J. Electron. Mater. 35 (2006) 663.
[29] I.A. Sussmann, Phys. Condens. Mater. 2 (1964) 146.
[30] I.A. Sussmann, J. Phys. Chem. Solids 28 (1964) 1643.
[31] M.P. Tonkonogov, V.Y. Medvedev, Sov. Phys. J. 30 (1987) 122.